ACS OMEGA

http://pubs.acs.org/journal/acsodf

Article

Quartz Crystal Microbalance Coated with Polyacrylonitrile/Nickel Nanofibers for High-Performance Methanol Gas Detection

Yadi Mulyadi Rohman, Riris Sukowati, Aan Priyanto, Dian Ahmad Hapidin,* Dhewa Edikresnha, and Khairurrijal Khairurrijal*

Cite This: *ACS Omega* 2023, 8, 13342−13351

Read Online

ACCESS | Metrics & More | Article Recommendations

ABSTRACT: This study describes a sensor based on quartz crystal microbalance (QCM) coated by polyacrylonitrile (PAN) nanofibers containing nickel nanoparticles for methanol gas detection. The PAN/nickel nanofibers composites were made via electrospinning and electrospray methods. The QCM sensors coated with the PAN/nickel nanofiber composite were evaluated for their sensitivities, selectivities, and stabilities. The morphologies and elemental compositions of the sensors were examined using a scanning electron microscope-energy dispersive X-ray. A Fourier Transform Infrared spectrometer was used to investigate the elemental bonds within the nanofiber composites. The QCM sensors coated with PAN/nickel nanofibers offered a high specific surface area to enhance the QCM sensing performance. They exhibited excellent sensing characteristics, including a high sensitivity of 389.8 ± 3.8 Hz/SCCM, response and recovery times of 288 and 251 s, respectively, high selectivity for methanol compared to other gases, a limit of detection (LOD) of about 1.347 SCCM, and good long-term stability. The mechanism of methanol gas adsorption by the PAN/nickel nanofibers can be attributed to intermolecular interactions, such as the Lewis acid−base reaction by PAN nanofibers and hydrogen bonding by nickel nanoparticles. The results suggest that QCM-coated PAN/nickel nanofiber composites show great potential for the design of highly sensitive and selective methanol gas sensors.

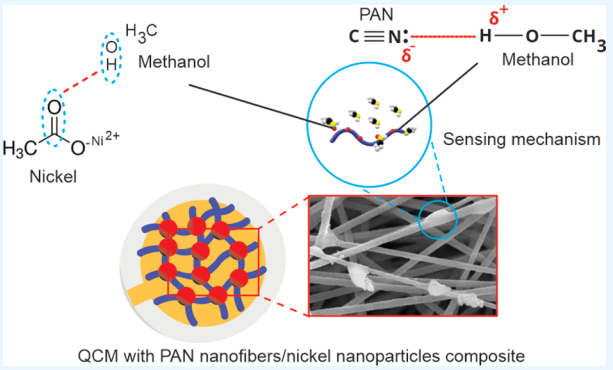

1. INTRODUCTION

Volatile organic compounds (VOC) gases, including ethanol, methanol, acetone, and formaldehyde, have recently attracted significant attention due to their potential harm to human health, even at low concentrations.[1,2] These compounds have been linked to a range of diseases, including respiratory disorders, cancer, anemia, and genotoxicity.[3,4] Among the VOCs, methanol (CH_3OH) is particularly prevalent in industrial[5] and medical[6] applications. However, its use poses a significant risk to human health, as exposure can cause blindness, headaches, and breathing difficulties.[7] An accurate detection method of methanol is then essential to prevent exposure.

Several methods have been developed for detecting methanol, including chemiresistive,[8] fiber optic,[9] chromatography,[10] and quartz crystal microbalance (QCM)[11] methods. However, these methods have limitations. For example, the chromatography method is expensive and requires complex equipment,[12] while the chemiresistive method is time-consuming and requires complex sample preparation.[13] The fiber optic method requires costly equipment and cannot be used for various colorless gas samples.[14] In addition, various materials have been developed for methanol sensing, such as Pd doped SnO_2 nanoparticles,[15] hollow hierarchical SnO_2-ZnO composite nanofibers,[16] Fe_2O_3-loaded NiO nanosheets,[17] and Al doped NiO nanofibers.[18] Despite previous works successfully improving methanol gas sensing performances of these materials, they still need high operating temperatures.

QCM-based gas sensors have attracted significant attentions in recent years due to their simple operation, low cost, and sensitivity, and because they operate at room temperature. QCM estimates the concentration of target gases by measuring the shift in resonance frequency when gas molecules accumulate on the sensor surface.[19] This sensor can also be modified to improve their sensing performance, such as sensitivity and selectivity, through various strategies, such as selecting suitable material and material structure for the

Received: February 6, 2023
Accepted: March 17, 2023
Published: March 28, 2023

https://doi.org/10.1021/acsomega.3c00760
ACS Omega 2023, 8, 13342−13351

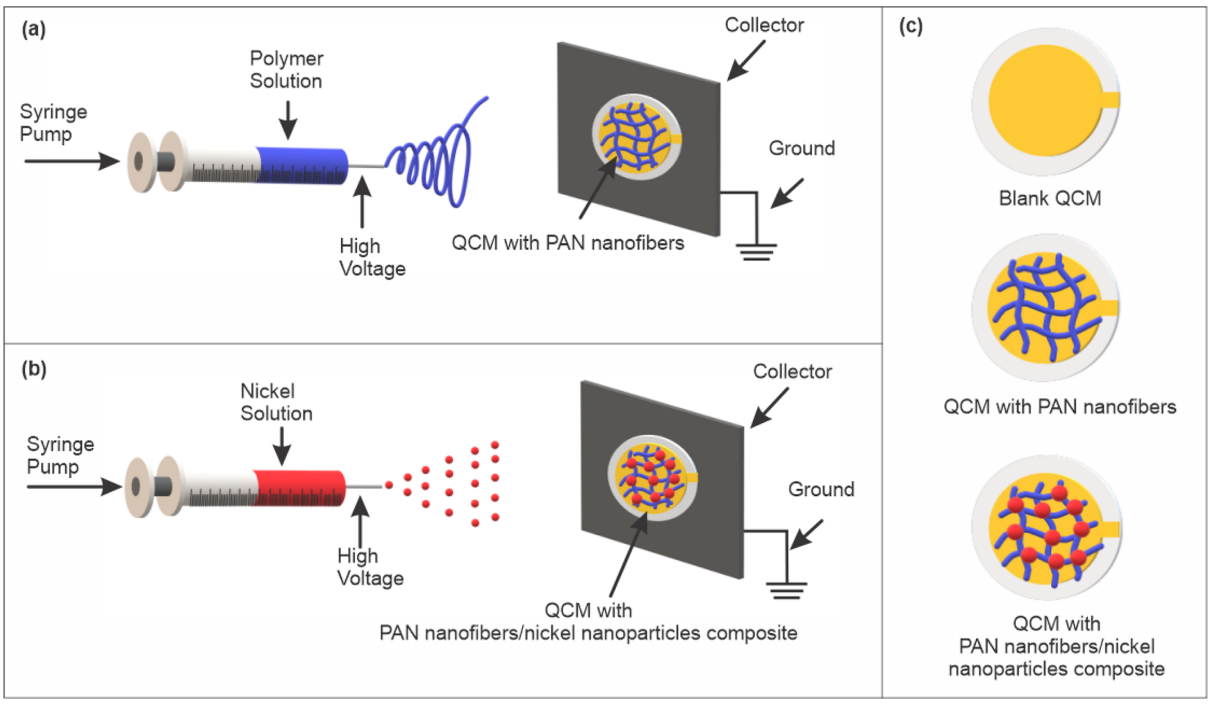

Figure 1. Schematic illustrations of (a) the electrospinning process of PAN nanofibers, (b) the electrospray process of nickel nanoparticles, and (c) the alteration of the QCM surface during the electrospinning and electrospray processes.

binding layer.[20] Various material structures have been used as the binding layer to enhance the QCM sensing performance, such as nanofibers,[21] thin films,[22] nanorods,[23] and nanoparticles.[24,25] Those materials' structures can be made from polymers, organic materials, or metal oxides. The utilization of metal oxides, such as nickel oxide (NiO),[26] zinc oxide (ZnO),[27] and tin oxide (SnO_2),[21] as gas sensor materials has been well established, and they have been shown to exhibit good performance. In particular, nickel (in the form of nickel acetate) has been used as a gas sensor material. For example, Simon et al. investigated the use of a graphene oxide composite with nickel nanoparticles as a gas sensor, and found that it exhibited good sensitivity to carbon monoxide, acetone, and nitrogen dioxide gases.[28] Additionally, the use of NiO in combination with SnO_2 as a toluene gas sensor has been investigated, and it has been found to be selective for toluene gas and exhibit a sensitivity that is 50 times higher than sensors without NiO. This enhanced performance is attributed to the intermolecular interaction of the gas with the binding layer of the QCM surface.[29]

Recently, polymeric electrospun nanofibers have gained significant attention as a binding layer material for gas sensors due to their large surface area and ability to be composited with various materials.[30] A variety of polymers, such as polyvinylpyrrolidone (PVP),[31] polyacrylonitrile (PAN),[32] and polyvinyl acetate (PVAc)[33] have been utilized as the binding layer of QCM sensors. Among these polymers, PAN nanofibers have been found to possess good mechanical stability, hydrophilicity, and insolubility in water, making them suitable as a composite matrix of the binding layer.[34] However, to date, there has no study been conducted on the development of a QCM binding layer consisting of PAN nanofibers and nickel nanoparticles for methanol sensing applications. Nickel has been shown to have good sensitivity for detecting toxic gases,[35] while the nanofibers structure provides a matrix with a high surface area-to-volume ratio, which can improve the sensing performance of gas sensors.[36] QCM sensors with a PAN/nickel nanofibers binding layer are expected to exhibit good performance. Therefore, this study aims to fabricate a nanofiber composite made of PAN nanofibers containing nickel nanoparticles prepared via electrospinning and electrospray methods. The characterization of the resulting nanofibers membrane and its performance for methanol gas sensing will also be discussed.

2. MATERIALS AND METHODS

2.1. Materials. PAN with a molecular weight of ~150,000 g/mol, nickel(II) acetate tetrahydrate, and *N*,*N*-dimethylformamide (DMF) were purchased from Sigma-Aldrich, Singapore. High-purity nitrogen gas was purchased from CV Sangkuriang, Indonesia. The test gases were the vapors of methanol, formaldehyde, acetone, ethanol, and water. Methanol and ethanol (99% purity) were purchased from Sigma-Aldrich, Singapore. Formaldehyde (95% purity) and acetone (95% purity) were purchased from ChemPro, Indonesia. QCM sensors (HC49U AT Cut) were supplied by PT.Great Microtama Electronic Indonesia (GXC), Indonesia. Prior to the sensing process, the QCM sensors were thoroughly cleaned by gently rinsing them with ethanol and acetone and then drying them in a dry box for a period of 24 h.

2.2. Sensor Preparations. PAN/nickel nanofibers composites were produced by electrospinning and electrospray techniques, which are schematically given in Figure 1a,b, respectively. At first, the PAN nanofibers were fabricated via electrospinning (ILMI-N101, Indonesia). Afterward, the electrospray process was carried out to make nickel nanoparticles using the same equipment in producing the nanofibers. The PAN precursor solution was initially prepared by dissolving 0.8 g of PAN powder in 10 mL of DMF solution using a magnetic stirrer at room temperature. The nickel

https://doi.org/10.1021/acsomega.3c00760
ACS Omega 2023, 8, 13342−13351

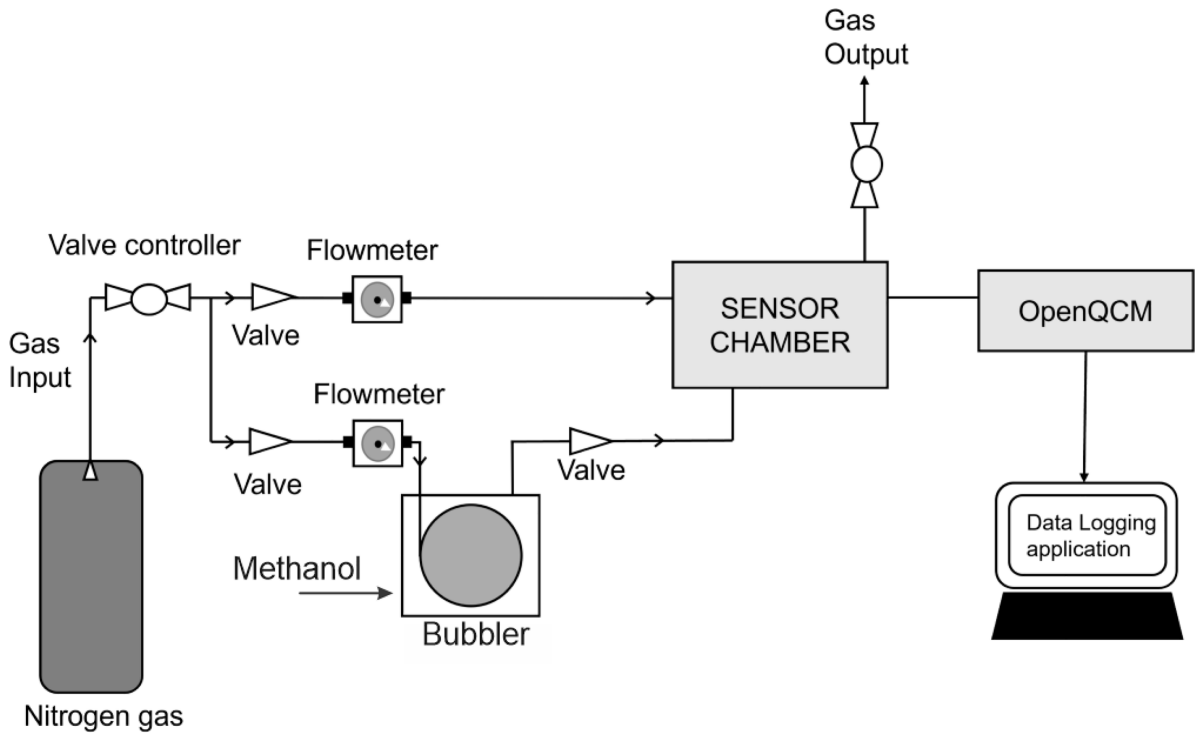

Figure 2. Sensing characterization of QCM with the PAN nanofiber/nickel nanoparticle composite for methanol gas detection.

solution was prepared by dissolving 0.8 g of nickel(II) acetate tetrahydrate in ethanol using a simple stirring method until it became homogenous. The PAN solution was inserted into a 10 mL syringe for electrospinning. The electrospinning process parameters were an applied voltage of 16 kV, a collector-to-needle tip distance of 15 cm, and a flowrate of 3−4 mL/h. The electrospray process parameters were an applied voltage of 16 kV, with a 1.8−3 mL/h flowrate at the tip-to-collector distance of 15 cm. PAN nanofibers were coated directly on the QCM attached to the grounded collector using the electrospinning process. Following the electrospinning process, the electrospun PAN nanofibers-coated QCM was sprayed with a small number of nickel nanoparticles using the electrospray process. The QCM with a modified surface layer is depicted in Figure 1c. After the electrospinning and electrospray processes were completed, the QCM coated by PAN/nickel nanofibers composite was then dried up for 24 h in a dry box chamber (Kris Dry Cabinet, Indonesia).

2.3. Materials Characterizations. The morphology, diameter distribution, and elemental composition of PAN/nickel nanofiber composites were analyzed using a scanning electron microscope (SEM) and energy dispersive spectroscopy (EDS) (JEOL, JSM-6510A/JSM-6510LA). A Fourier-transform infrared spectroscope (FTIR) (Bruker, Alpha Platinum ATR A220/D-01) was employed to analyze chemical bonds and functional groups of PAN/nickel nanofibers. Their crystallization characteristics were determined by an X-ray diffractometer (PANanalytical X-ray diffraction E'xpert Pro 3040/x0). The resonant frequency shifting of QCM was measured using OpenQCM (Wi2, OpenQCM).

2.4. Sensor Characterizations for Methanol Detection. Sensing of methanol gas using a PAN/nickel nanofiber-based QCM sensor is illustrated in Figure 2. A nitrogen gas was used to generate vapor from solutions[37] and clean a closed chamber containing the QCM device. The desired flow rate of the analyte gas was adjusted using a flow meter. The flow meter controlled the flow of both the nitrogen gas into the bubbler and directly into the sensor chamber for cleaning purposes. In the bubbler, methanol vapor was produced and then transported to the sensor chamber with the regulated flow rate. The QCM was positioned in the sensor chamber, connected to the OpenQCM, and a voltage of 5 V was applied to record the resonant frequency. The sensor response was determined by exposing it to methanol vapor carried by nitrogen gas at various continuous flow rates ranging from 400 to 1600 SCCM. The temperature and relative humidity inside the test chamber were recorded as 24.6 ± 0.1 and 37.6 ± 3.5%, respectively. Theoretically, the resonant frequency change is proportional to the deposited mass, which is given by the Sauerbrey equation:

$$\Delta f = -\frac{2f_0^2}{A\sqrt{\rho_0\mu_0}}\Delta m \quad (1)$$

where Δf is the change in the resonant frequency of QCM (Hz), f_0 is the fundamental frequency of QCM (5 MHz), Δm is the deposited mass (ng), A is the active surface area of the QCM electrode, and ρ_0 and μ_0 are the shear modulus and density of quartz crystals, respectively.

In this study, several sensor parameters were evaluated, including an optimum flowrate, response and recovery dynamics, sensitivity, limit of detection (LOD), limit of quantification (LOQ), selectivity, and stability. The response time was defined as the time required for the adsorption process, characterized by the absence of a reduced resonant frequency. Recovery time was defined as the time required to return the frequency to its initial state. The sensor sensitivity was defined as the ratio of the frequency shift to the target gas flow rate. Additionally, the standard deviation of the blank measurements and the gradient of the plot of the frequency

https://doi.org/10.1021/acsomega.3c00760
ACS Omega 2023, 8, 13342−13351

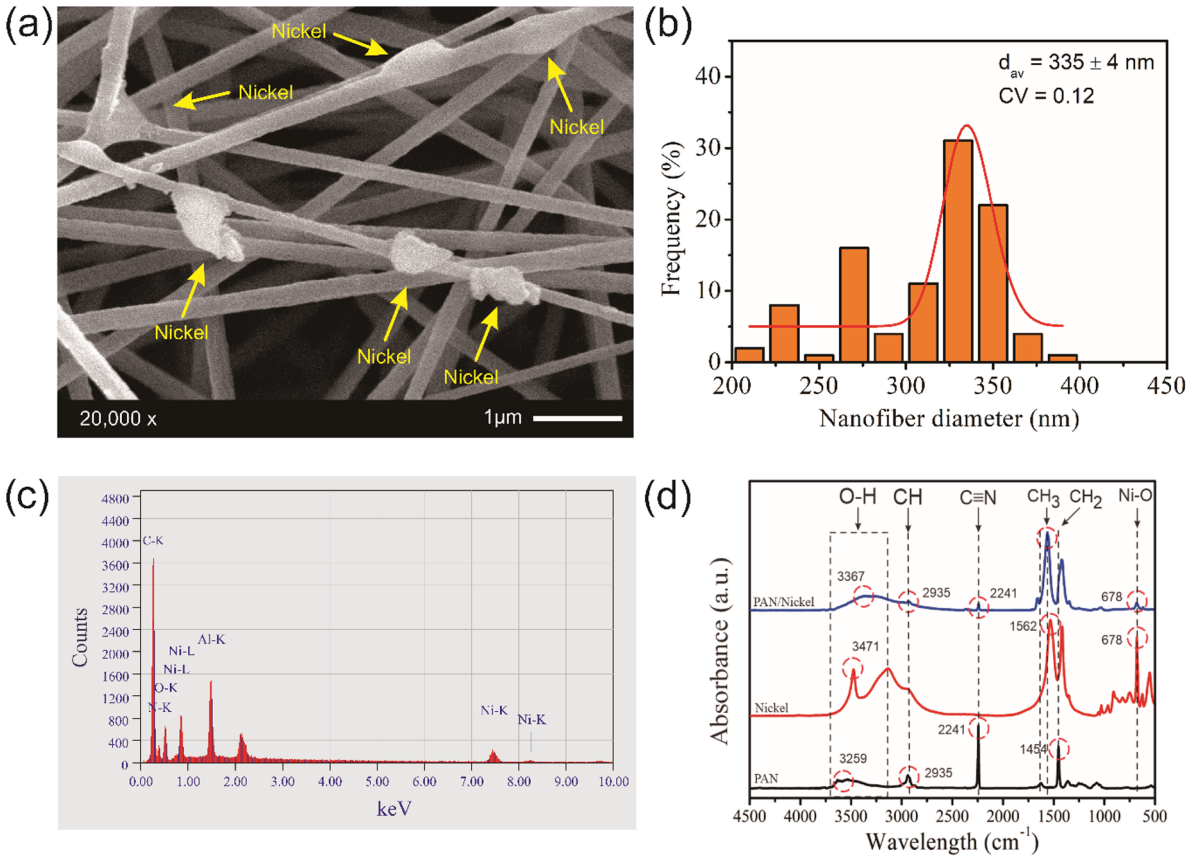

Figure 3. SEM image of (a) PAN/nickel nanofibers deposited on QCM, (b) nanofiber diameter distribution of PAN/nickel nanofibers deposited on QCM, (c) EDX analysis of PAN/nickel nanofibers, and (d) FTIR spectra of PAN, nickel nanoparticles, and PAN/nickel nanofibers.

shift against analyte concentration can be used to estimate LOD and LOQ.[38] A sensitive sensor is considered to have a low LOD and LOQ. LOD refers to the lowest amount of a substance that can be detected by the sensor, while LOQ refers to the lowest amount that can be accurately quantified. A lower LOD and LOQ indicate a higher sensitivity and precision of the sensor. The ability of the sensor was evaluated after it was used in methanol sensing for 1 month. Furthermore, selectivity was employed to ensure that the QCM sensor did not produce false positive results with another gas.

3. RESULTS AND DISCUSSION

3.1. Sample Characterizations. The PAN/nickel nanofibers coated QCM was successfully developed. Figure 3a presents SEM images of PAN/nickel nanofibers in which nickel nanoparticles agglomerated, as indicated by the yellow arrows. The PAN/nickel nanofibers have a high ratio of length to diameter, and it is shown that nickel nanoparticles were randomly piled up on the nanofibers. The estimated average diameter of PAN/nickel nanofibers was found to be (335 ± 4) nm, exhibiting a relatively homogeneous, smooth, and continuous structure, as given in Figure 3b.

Figure 3c depicts EDX analysis of the PAN/nickel nanofibers collected on the aluminum foil. It reveals peaks for elements such as C, O, N, Ni, and Al, with C and N being the main elements found in PAN nanofibers $(C_3H_3N)_n$.[32] The Ni and O peaks indicate the presence of nickel and oxygen in the composite $(C_4H_{14}NiO_8)$. The Al peak is a result of the PAN/nickel composite being deposited on the surface of the aluminum foil collector. The most prominent carbon element was seen at C, with 50% formed by PAN and acetate. The nitrogen content appeared at 23% in the nitrile chain of PAN, and the elemental oxygen was seen at 13%, representing the essential oxygen in nickel(II) acetate tetrahydrate. The mass basic content of nickel in the PAN/nickel nanofibers was 8.07%. The SEM images and EDX analyses proved that the composite consists of PAN nanofibers and nickel nanoparticles.

The FTIR spectra, as shown in Figure 3d, confirmed the presence of agglomerated nickel nanoparticles on the PAN nanofibers as previously indicated by SEM−EDX analyses. The spectra revealed the existence of O−H groups in the PAN/nickel nanofibers, indicated by the peak at 3367 cm^{-1}, which originated from the hydroxyl bond that was more pronounced with the increase in phenol groups. It was characterized by a wide absorption spectrum of PAN/nickel nanofiber and a shifted of the O−H groups.[39] The FTIR spectra also showed the presence of C−H groups in the PAN/nickel composite, with the stretching vibration band appearing at 2935 cm^{-1}. However, the peak absorbance of this band was smaller in the composite compared to pure PAN, indicating that the presence of C−H groups was influenced by the addition of nickel acetate.[40] The nitrile group C≡N appeared at 2241 cm^{-1} with a smaller absorbance value than pure PAN.[41]

The FTIR spectra also showed the presence of a carbonyl group and asymmetric bending −CH3 of nickel acetate,[26] indicated by the stretching band at 1562 cm^{-1}. Stretching at 1454 cm^{-1} indicated the presence of asymmetric $-CH_2$ aliphatic groups owned by PAN The peak absorbance at 678 cm^{-1} denoted the presence of a Ni−O bond group,[42] while the

https://doi.org/10.1021/acsomega.3c00760
ACS Omega 2023, 8, 13342−13351

C═O vibration indicated the peak at 1673 cm^{-1}, which is typically a strong band in DMF.[43] However, the PAN/nickel composite still formed as indicated by the peak at 1660 cm^{-1} with a small absorbance, showing that the electrospinning process effectively evaporated the solvent. The FTIR spectra of PAN/nickel nanofiber composites revealed that a bond was formed between PAN and nickel acetate through intermolecular interactions between the O−H groups in nickel acetate and the C≡N groups in PAN.

The crystalline structure of samples was analyzed using XRD. Figure 4 displays the XRD patterns of the PAN powder

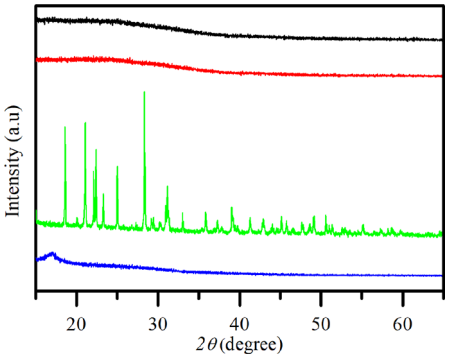

Figure 4. XRD patterns of PAN powder (blue line), nickel powder (green line), PAN nanofibers (red line), and PAN/nickel nanofibers (black line).

(blue line), nickel powder (green line), PAN nanofibers (red line), and PAN/nickel nanofibers (black line). The diffraction peak of PAN, at 16.55°, reveals its crystalline nature.[44] The primarily amorphous nature of PAN nanofibers and PAN/nickel can be linked to pure PAN polymer. The nickel sample (green line) was found to have a crystalline structure with peaks at 2θ = 44.53, 45.01, 70.82, and 71.76°.[45] The peak of PAN/nickel nanofibers was assigned at 24.11°, which is a peak of PAN nanofibers, and with peaks at 22.99, 33.50, 38.50, 44.74, and 65.26°, which are peaks of nickel.[46] The presence of nickel nanoparticles could significantly catalyze the transformation of polymeric nanofibers into a carbon-like graphite structure upon annealing in an argon atmosphere.[47]

3.2. Responses of PAN/Nickel-Nanofibers Coated QCM Sensors. Response testing was conducted on four types of QCM sensors: blank QCM (QCM without an active layer), QCM PAN (QCM with PAN nanofiber active layer), QCM nickel (QCM with nickel nanoparticle active layer), and QCM PAN/nickel (QCM with PAN/nickel nanofiber active layer). The response was tested using the bubbler method,[48] and the frequency shift was measured with gas flow rates ranging from 400 to 1600 SCCM with five-cycle dynamic responses.

The frequency shift for blank QCM (figure 5a), QCM PAN (figure 5b), QCM nickel (figure 5c), and QCM PAN/nickel (figure 5d) were 6.9, 62.3, 157.4, and 437.9 Hz, respectively. The frequency shift increased with the gas flow rate for all sensors, with the highest response observed in the QCM PAN/nickel sensor. The resonant frequency shift was three times higher in the QCM PAN/nickel sensor compared to the QCM nickel sensor and eight times higher compared to the QCM PAN sensor. These results indicate that the active layer of PAN/nickel nanofibers can significantly enhance the QCM sensor response.

The mechanism of response and recovery in the QCM sensor with PAN/nickel nanofibers was investigated for methanol gas. The repeatability of the response was tested for five cycles to assess reversibility. The response time was optimized at 300 s and was affected by the flow rate of nitrogen gas as clean air. The response time for the QCM PAN/nickel sensor was longer than the other sensors, with obtained response times of 120, 249, 259, and 288 s for blank QCM, QCM PAN, QCM nickel, and QCM PAN/nickel, respectively. This response time dramatically affects the active layer on the QCM surface. Although the blank QCM had a fast response time, it was unstable in the detection of analyte gases. In contrast, the QCM PAN, QCM nickel, and QCM PAN/nickel sensors had good responses to methanol gas even with their longer response times. The adsorption ability of the active layers on the QCM surface depends on the response time, and this desorption time affects the number of molecules that bind to the active layer.

In Figure 5e, the dynamic response of QCM sensors with various gas flow rates ranging from 400 to 1600 SCCM is shown, along with the five-cycle dynamic responses. The recovery times for the blank QCM, QCM with PAN nanofibers, QCM with nickel nanoparticles, and QCM with PAN/nickel nanofibers were 56, 107, 143, and 251 s, respectively. These results were found to be directly proportional to the number of adsorbed molecules on the surface of the active layer. The more the molecules are absorbed, the lower the resonant frequency, resulting in a longer bond time for the active layer to desorb the analyte gas molecules. In comparison to previous studies of QCM as a methanol sensor, the QCM with PAN/nickel nanofibers was found to be much better for sensing methanol gas. For example, the study by Nugroho et al. found that the QCM with cellulose acetate/chitosan was only able to reduce the resonant frequency to <10 Hz.[49] Similarly, Rianjanu et al. modified a QCM sensor with PVAc nanofiber for the detection of alcohol vapor, where the sensor is capable of reducing the resonant frequency by <25 Hz.[50] The results of the cycling tests showed excellent repeatability of response, with methanol molecules rapidly desorbed after purging with nitrogen gas and the frequency returning to its initial value.

3.3. Sensitivities of PAN/Nickel Nanofiber-Coated QCM Sensors. The sensitivity of QCM sensors was determined by analyzing the gradient of a linear function that fit the frequency shift vs the flow rate graph.[50] The testing of QCM sensors was performed in the operating range of flow rates from 400 to 1600 SCCM. The sensitivity of the QCM sensors is depicted in Figure 6. The blank QCM sensor was described by the equation $y = 6.2x + 1.84$ with a determination correlation of R^2 = 0.921. The frequency response exhibited good linearity, as indicated by R^2 values greater than 0.994 for the various sensors. Additionally, the determination correlation for the blank QCM sensor had a relatively low value, signifying that the sensor was less sensitive to methanol gas, with a sensitivity value of 6.2 Hz/SCCM. Upon similar analysis, the sensitivity values were found to be 40.7, 152.8, and 389.8 Hz/SCCM for QCM sensors with PAN nanofibers, nickel nanoparticles, and PAN/nickel nanofibers, respectively. It was evident that the QCM sensor with PAN/nickel was the most sensitive to methanol compared to other ones.

The LOD and LOQ of the modified QCM sensors were calculated using eqs 2 and 3, respectively,[51] as follows:

https://doi.org/10.1021/acsomega.3c00760
ACS Omega 2023, 8, 13342−13351

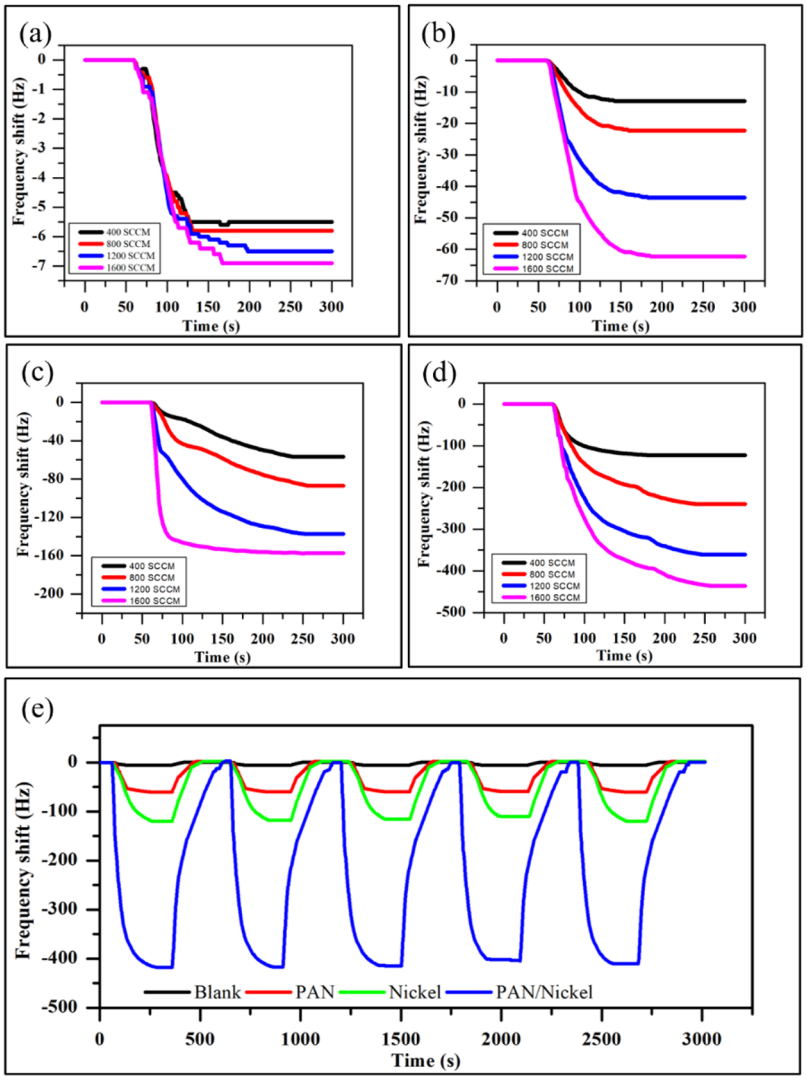

Figure 5. Response of sensor QCM for (a) blank QCM, (b) QCM PAN, (c) QCM nickel, and (d) QCM PAN/nickel exposed with various gases flowrate at room temperature. (e) Response of sensors for five-cycle dynamic responses (reversibility) of the blank QCM, QCM PAN, QCM nickel, and QCM PAN/nickel sensors exposed to 1600 SCCM methanol gas at room temperature.

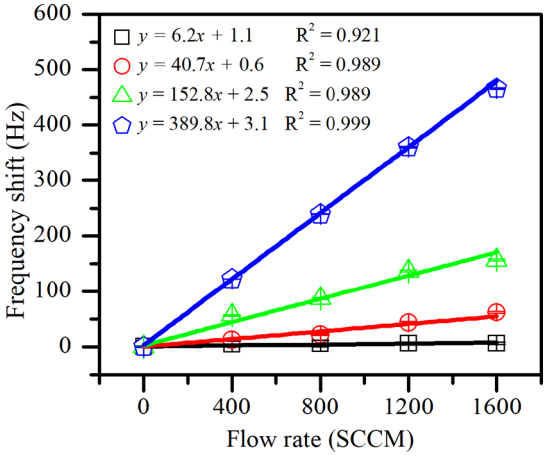

Figure 6. Sensitivity of QCM sensors at various flow rates.

$$\mathrm{LOD} = 3.3\frac{\sigma}{S} \tag{2}$$

$$\mathrm{LOQ} = 10\frac{\sigma}{S} \tag{3}$$

where σ is standard deviation of the blank QCM and S is the sensitivity of sensor (Hz/SCCM). The calculated LOD and LOQ values of the QCM for methanol detection are presented in Table 1. The highest LOD and LOQ values were obtained using the blank QCM, while the lowest were obtained with the QCM PAN/nickel.

3.4. Stabilities and Selectivities of PAN/Nickel Nanofiber-Coated QCM Sensors. The long-term stability of the QCM sensors was evaluated by regularly testing them for

Table 1. Performance of QCM Sensors

QCM	frequency shift (Hz)	sensitivity (Hz/SCCM)	R^2	LOD (SCCM)	LOQ (SCCM)
blank	6.9	6.2 ± 1.9	0.921	4.348	13.178
PAN	62.3	40.7 ± 2.9	0.989	2.346	7.108
nickel	157.4	152.8 ± 8.6	0.989	2.131	6.461
PAN/nickel	465.7	389.8 ± 3.8	0.999	1.347	4.083

https://doi.org/10.1021/acsomega.3c00760
ACS Omega 2023, 8, 13342−13351

methanol gas over a period of 30 days. The results, shown in Figure 7, indicate that the QCM sensors exhibit good stability,

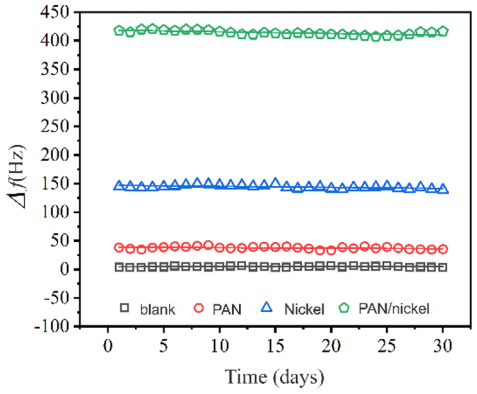

Figure 7. Long-term stability of sensors response at 1600 SCCM of methanol gases during 30 days of measurements.

with maximum frequency fluctuations of 2.9 Hz for the blank QCM, 4.0 Hz for the QCM PAN, 4.0 Hz for the QCM nickel, and 2.9 Hz for the QCM PAN/nickel. These results demonstrate the good stability of the QCM sensor with PAN/nickel nanofibers.

To evaluate the selectivity of the QCM sensor coated with PAN/nickel nanofibers toward methanol gas, the sensor was exposed to various gases, including methanol, acetone, formaldehyde, water, and a mixture of gases, with a flow rate ranging from 400 to 1600 SCCM. The adsorption selectivity was further evaluated by exposing the QCM to different gases commonly found as toxic and air pollutants,[39,41,42,52] such as ethanol, acetone, formaldehyde, and water. The results, shown in Figure 8, indicate that the QCM sensor with PAN/nickel nanofibers had a higher frequency reduction for methanol gas, with a frequency shift of 465.7 ± 7.2 Hz. In comparison, the frequency shifts for other gases were as follows: ethanol (52.1 ± 1.4 Hz), formaldehyde (10.2 ± 1.4 Hz), acetone (15.2 ± 1.5 Hz), water (29.8 ± 2.3 Hz), and mixture gas (29.8 ± 2.3 Hz). The selectivity was further verified by comparing the frequency shift to that of free air, which showed lower frequency shifts for methanol (387.9 ± 1.5 Hz), ethanol (45.1 ± 1.8 Hz), formaldehyde (5.1 ± 1.7 Hz), acetone (13.2 ± 1.9 Hz), water (18.2 ± 0.2 Hz), and mixture gas (25.8 ± 0.2 Hz). These results demonstrate the ability of the QCM sensor with PAN/nickel nanofibers to detect methanol gas with high selectivity. The minimum detection concentration for methanol was determined by testing the sensor's response using the vapor method and a calibration curve between frequency change and concentration, which showed that the QCM PAN/nickel can detect methanol from 7 to 550 ppm. In comparison with existing methanol sensors using different types of sensors, materials, and morphologies (as listed in Table 2), our methanol sensor demonstrates exceptional performance with good response at room temperature (24.6 °C).

3.5. Sensing Mechanism of PAN/Nickel Nanofiber-Coated QCM Sensors. The interaction of methanol gas with the QCM sensor coated with PAN/nickel nanofibers is strong, as demonstrated in Figure 9. The reversible intermolecular interaction between PAN, nickel, and methanol serves as the sensing mechanism. PAN polymers have a nitrogen atom that acts as a Lewis base and a hydrogen atom that acts as a Lewis acid due to its electron deficiency. The lone pair of electrons in each PAN polymer subunit interacts strongly with the proton in the hydrogen group of the methanol molecule, leading to a strong bond and a decrease in the resonance frequency of the QCM, indicating mass deposition on the QCM surface due to the bond between the PAN nanofibers and the methanol analyte gas.[37] Similarly, the nickel nanoparticles also participate in intermolecular interactions, as the nickel(II) acetate tetrahydrate contains a carbonyl group in its acetate structure, forming hydrogen bonds with the hydroxyl group in the methanol molecule.

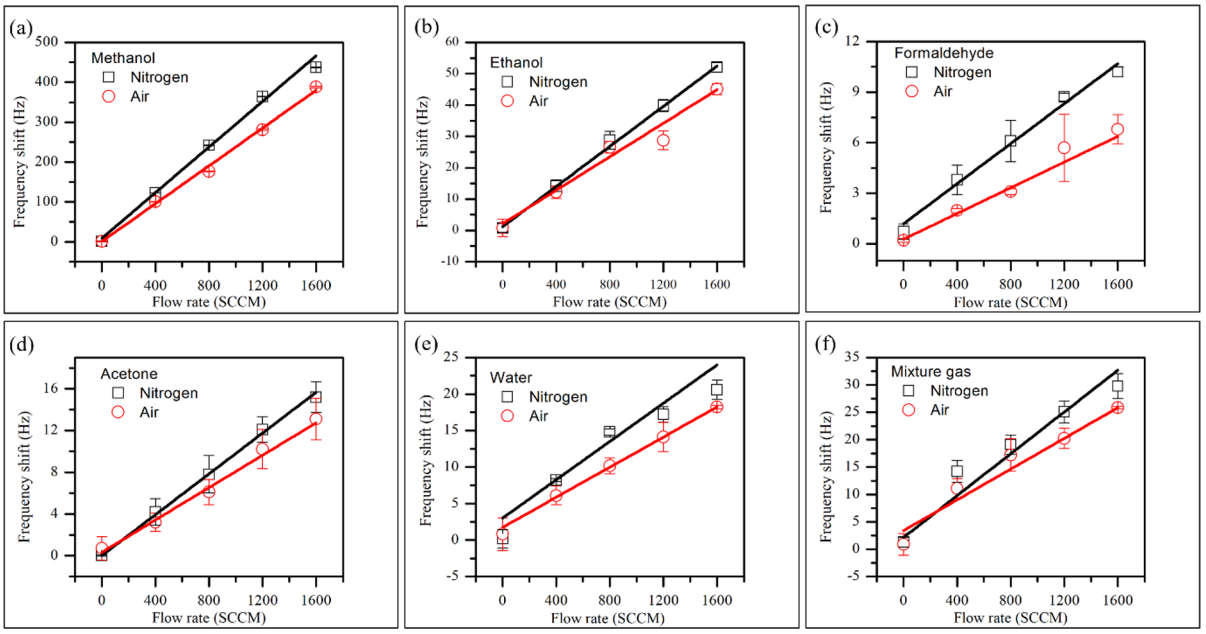

Figure 8. Frequency shift of the QCM sensor with PAN/nickel nanofibers when exposed to various gases with various flow rates, to evaluate the performance of the selectivity sensor for (a) methanol, (b) ethanol, (c) formaldehyde, (d) acetone, (e) water, and (f) mixture gas.

https://doi.org/10.1021/acsomega.3c00760
ACS Omega 2023, 8, 13342−13351

Table 2. Properties of Methanol Sensor Based on Various Materials

type of sensors	materials	morphology	operation temperature	sensitivity/ response	response/recovery time	range of concentration	ref
QCM	PVAc	thin film		0.07 Hz/ppm		500−3000 ppm	34
QCM	MIL101 (Cr)	nanoporous		0.306 Hz/ppm		5−700 ppm	53
QCM	PVAc	nanofiber		0.01 Hz/ppm		50 ppm	54
QCM	PVAc	nanofiber		0.5 Hz/ppm		0.5−4 mg/L	33
chemoresistive	Pd doped SNO_2	nanoparticle	350 °C	10	102 s	5−1000 ppm	15
metal oxide semiconductor	Ag-$LaFeO_3$	fiber	125−175 °C	-	45/33 s	5 ppm	55
metal oxide semiconductor	SnO_2-ZnO	nanofibers	350 °C	2.5−65	20/40 s	1−500 ppm	16
metal oxide semiconductor	Fe_2O_3 loaded NiO	nanosheet	255 °C	107.9	0.5/14.6 s	6.82−200 ppb	17
chemical sensor	Al doped NiO	nanofiber	325 °C	10.4	199 s/15 s	10.4−200 ppm	18
QCM	PAN/Ni	nanofiber	24.6 °C	390 Hz/SCCM	288/251 s	7−550 ppm	this Work

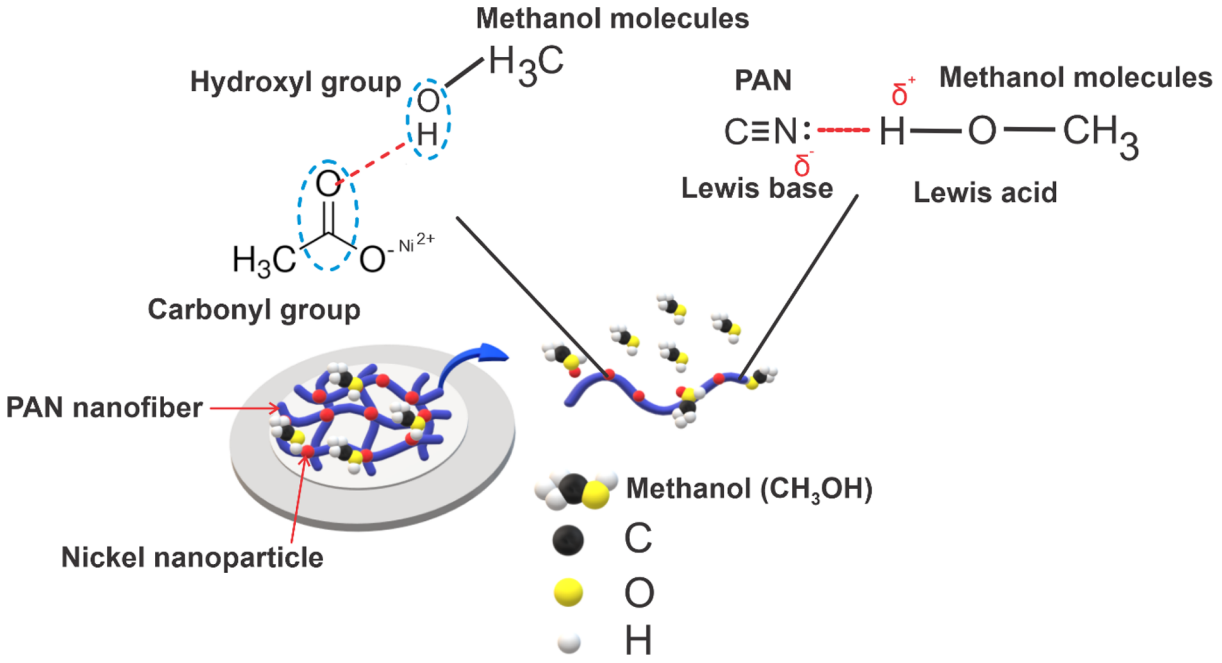

Figure 9. Interaction mechanism between the PAN/nickel composite and methanol gas on the surface of QCM.

The hydrogen bond between the methanol and nickel(II) acetate molecules is illustrated in Figure 9. The carbonyl group in nickel(II) acetate, consisting of two oxygen atoms, functions as a hydrogen acceptor. Conversely, the hydroxyl group in methanol, marked by the presence of OH, interacts with =CO in nickel(II) acetate. In this bond, methanol acts as the proton donor and nickel(II) acetate as the proton acceptor,[50] as indicated by the FTIR spectrum and EDS results. Intermolecular interactions, particularly hydrogen bonds, occur when the sensor's active layer is exposed to methanol gas, reducing the resonant frequency and increasing the mass deposited on the QCM surface. This increase in mass, seen in SEM results, shows the number of molecules adsorbed on the QCM surface, thus increasing the sensor's sensitivity to methanol gas. The presence of nickel nanoparticles on the surface of PAN nanofibers enhances the sensor's absorption surface area, and the optimum flow rate is 1600 SCCM, marked by no decrease in resonant frequency when the flow rate increases, indicating the limit of the QCM's binding capacity for methanol gas.

4. CONCLUSIONS

PAN/nickel nanofibers were successfully fabricated using the electrospinning and electrospray methods and utilized as the active layer of a QCM sensor for methanol detection. Characterization techniques, such as SEM, EDS, FTIR, and XRD, confirmed the presence of nickel nanoparticles on the surface of PAN nanofibers and the formation of chemical bonds between them. The QCM sensor with PAN/nickel nanofibers demonstrated significantly improved sensitivity to methanol gas with a response of 389.8 Hz/SCCM, as well as low LOD and LOQ. The sensor also displayed high selectivity toward methanol gas and fast response and recovery times. The enhanced sensitivity of the sensor is attributed to Lewis' acid−base reactions and hydrogen bonding. Additionally, the sensor demonstrated long-term stability. This work provides a promising alternative for methanol detection.

AUTHOR INFORMATION

Corresponding Authors

Dian Ahmad Hapidin − *Department of Physics, Faculty of Mathematics and Naturals Sciences, Institut Teknologi*

https://doi.org/10.1021/acsomega.3c00760
ACS Omega 2023, 8, 13342−13351

Bandung, Bandung, West Java 40132, Indonesia; Email: hapidin@fi.itb.ac.id

Khairurrijal Khairurrijal − *Department of Physics, Faculty of Mathematics and Naturals Sciences, Institut Teknologi Bandung, Bandung, West Java 40132, Indonesia; Research Center for Biosciences and Biotechnology, University Center of Excellence-Nutraceutical, Institut Teknologi Bandung, Bandung, West Java 40132, Indonesia; Department of Physics, Faculty of Science, Institut Teknologi Sumatera, Lampung 35365, Indonesia*; orcid.org/0000-0002-9452-4192; Email: krijal@office.itb.ac.id

Authors

Yadi Mulyadi Rohman − *Department of Physics, Faculty of Mathematics and Naturals Sciences, Institut Teknologi Bandung, Bandung, West Java 40132, Indonesia*; orcid.org/0000-0002-0685-9022

Riris Sukowati − *Department of Physics, Faculty of Mathematics and Naturals Sciences, Institut Teknologi Bandung, Bandung, West Java 40132, Indonesia*

Aan Priyanto − *Department of Physics, Faculty of Mathematics and Naturals Sciences and Doctoral Program of Physics, Faculty of Mathematics and Naturals Sciences, Institut Teknologi Bandung, Bandung, West Java 40132, Indonesia*; orcid.org/0000-0002-7553-6446

Dhewa Edikresnha − *Department of Physics, Faculty of Mathematics and Naturals Sciences, Institut Teknologi Bandung, Bandung, West Java 40132, Indonesia; Research Center for Biosciences and Biotechnology, University Center of Excellence-Nutraceutical, Institut Teknologi Bandung, Bandung, West Java 40132, Indonesia*; orcid.org/0000-0001-6203-4343

Complete contact information is available at: https://pubs.acs.org/10.1021/acsomega.3c00760

Author Contributions

Y.M.R. contributed to conceptualization, methodology, writing-original draft, and data curation. R.S., and A.P. contributed to conceptualization, methodology, and data curation. D.A.H. and D.E. contributed to resources and supervision. K.K. contributed to resources, writing−review, editing, supervision, and funding acquisition.

Notes

The authors declare no competing financial interest.

■ ACKNOWLEDGMENTS

This research was financially supported by the Institute for Research and Community Service, ITB Research Grant in the fiscal year 2020-2022, Institute for Research and Community Engagement (LPPM-ITB), through P3MI Research program 2020 and Indonesia Endowment Fund for Education (LPDP) scholarship for R.S. and A.P. We gratefully acknowledge the Basic Science Center A ITB for SEM analysis.

■ REFERENCES

(1) Wang, H.; Zhang, Y.; Zhao, H.; Lu, X.; Zhang, Y.; Zhu, W.; Nielsen, C. P.; Li, X.; Zhang, Q.; Bi, J.; McElroy, M. B. Trade-Driven Relocation of Air Pollution and Health Impacts in China. *Nat. Commun.* **2017**, *8*, 738.

(2) Jin, P.; Wang, T.; Liu, N.; Dupont, S.; Beardall, J.; Boyd, P. W.; Riebesell, U.; Gao, K. Ocean Acidification Increases the Accumulation of Toxic Phenolic Compounds across Trophic Levels. *Nat. Commun.* **2015**, *6*, 8714.

(3) Kivrak, E.; Ince-yardimci, A.; Ilhan, R.; Kirmizibayrak, P. B.; Yilmaz, S.; Kara, P. Aptamer-Based Electrochemical Biosensing Strategy toward Human Non-Small Cell Lung Cancer Using Polyacrylonitrile. *Polypyrrole Nano.* **2020**, 7851−7860.

(4) Bartzis, J.; Wolkoff, P.; Stranger, M.; Efthimiou, G.; Tolis, E. I.; Maes, F.; Nørgaard, A. W.; Ventura, G.; Kalimeri, K. K.; Goelen, E.; Fernandes, O. On Organic Emissions Testing from Indoor Consumer Products' Use. *J. Hazard. Mater.* **2015**, *285*, 37−45.

(5) Park, J. Y.; Kwak, Y.; Lim, H.-R.; Park, S.-W.; Lim, M. S.; Cho, H.-B.; Myung, N. V.; Choa, Y.-H. Tuning the Sensing Responses towards Room-Temperature Hypersensitive Methanol Gas Sensor Using Exfoliated Graphene-Enhanced ZnO Quantum Dot Nanostructures. *J. Hazard. Mater.* **2022**, *438*, No. 129412.

(6) Hu, Q.; Huang, B.; Li, Y.; Zhang, S.; Zhang, Y.; Hua, X.; Liu, G.; Li, B.; Zhou, J.; Xie, E.; Zhang, Z. Methanol Gas Detection of Electrospun CeO2 Nanofibers by Regulating Ce3+/ Ce4+ Mole Ratio via Pd Doping. *Sens. Actuators, B* **2020**, *307*, No. 127638.

(7) Zhu, L.; Zeng, W.; Ye, H.; Li, Y. Volatile Organic Compound Sensing Based on Coral Rock-like ZnO. *Mater. Res. Bull.* **2018**, *100*, 259−264.

(8) Sinha, M.; Neogi, S.; Mahapatra, R.; Krishnamurthy, S.; Ghosh, R. Material Dependent and Temperature Driven Adsorption Switching (p- to n- Type) Using CNT/ZnO Composite-Based Chemiresistive Methanol Gas Sensor. *Sens. Actuators, B* **2021**, *336*, No. 129729.

(9) Maricar, M. M. S.; Sastikumar, D.; Reddy Vanga, P.; Ashok, M. Fiber Optic Gas Sensor Response of Hydrothermally Synthesized Nanocrystalline Bismuth Tungstate to Methanol. *Mater. Lett.* **2021**, *288*, No. 129337.

(10) Yassin, M. F.; Pillai, A. M. Monitoring of Volatile Organic Compounds in Different Schools: A Determinant of the Indoor Air Quality. *Int. J. Environ. Sci. Technol.* **2019**, *16*, 2733−2744.

(11) Sun, L.-X.; Okada, T. Simultaneous Determination of the Concentration of Methanol and Relative Humidity Based on a Single Nafion(Ag)-Coated Quartz Crystal Microbalance. *Anal. Chim. Acta* **2000**, *421*, 83−92.

(12) Samide, M. J.; Smith, G. D. Analysis and Quantitation of Volatile Organic Compounds Emitted from Plastics Used in Museum Construction by Evolved Gas Analysis − Gas Chromatography − Mass Spectrometry. *J. Chromatogr. A* **2015**, *1426*, 201−208.

(13) Moon, H. G.; Han, S. D.; Kang, M.; Jung, W.; Jang, H. W.; Yoo, K. S.; Park, H.; Kang, C. Y. *Chemiresistive Sensor Array Based on Semiconducting Metal Oxides for Environmental Monitoring*. 2014, *23* (1), 15−18, DOI: 10.5369/JSST.2014.23.1.15.

(14) Mayorga-Martinez, C. C.; Cadevall, M.; Guix, M.; Ros, J.; Merkoçi, A. Bismuth Nanoparticles for Phenolic Compounds Biosensing Application. *Biosens. Bioelectron.* **2013**, *40*, 57−62.

(15) van den Broek, J.; Abegg, S.; Pratsinis, S. E.; Güntner, A. T. Highly Selective Detection of Methanol over Ethanol by a Handheld Gas Sensor. *Nat. Commun.* **2019**, *10*, 4220.

(16) Tang, W.; Wang, J.; Yao, P.; Li, X. Hollow Hierarchical SnO2-ZnO Composite Nanofibers with Heterostructure Based on Electrospinning Method for Detecting Methanol. *Sens. Actuators, B* **2014**, *192*, 543−549.

(17) Tan, W.; Tan, J.; Fan, L.; Yu, Z.; Qian, J.; Huang, X. Fe2O3-Loaded NiO Nanosheets for Fast Response/Recovery and High Response Gas Sensor. *Sens. Actuators, B* **2018**, *256*, 282−293.

(18) Feng, C.; Jiang, Z.; Chen, B.; Cheng, P.; Wang, Y.; Huang, C. Aluminum-Doped NiO Nanofibers as Chemical Sensors for Selective and Sensitive Methanol Detection. *Anal. Methods* **2019**, *11*, 575−581.

(19) Zhang, D.; Wang, D.; Li, P.; Zhou, X.; Zong, X.; Dong, G. Facile Fabrication of High-Performance QCM Humidity Sensor Based on Layer-by-Layer Self-Assembled Polyaniline/Graphene Oxide Nanocomposite Film. *Sens. Actuators, B* **2018**, *255*, 1869−1877.

(20) Joshi, N.; Hayasaka, T.; Liu, Y.; Liu, H.; Oliveira, O. N.; Lin, L. A Review on Chemiresistive Room Temperature Gas Sensors Based on Metal Oxide Nanostructures, Graphene and 2D Transition Metal Dichalcogenides. *Microchim. Acta* **2018**, *185*, 213.

(21) Kang, Z.; Zhang, D.; Li, T.; Liu, X.; Song, X. Polydopamine-Modified SnO2 Nanofiber Composite Coated QCM Gas Sensor for High-Performance Formaldehyde Sensing. *Sens. Actuators, B* **2021**, *345*, No. 130299.
(22) Kumar, A.; Brunet, J.; Varenne, C.; Ndiaye, A.; Pauly, A.; Penza, M.; Alvisi, M. Tetra-Tert-Butyl Copper Phthalocyanine-Based QCM Sensor for Toluene Detection in Air at Room Temperature. *Sens. Actuators, B* **2015**, *210*, 398−407.
(23) Yan, D.; Xu, P.; Xiang, Q.; Mou, H.; Xu, J.; Wen, W.; Li, X.; Zhang, Y. Polydopamine Nanotubes: Bio-Inspired Synthesis{,} Formaldehyde Sensing Properties and Thermodynamic Investigation. *J. Mater. Chem. A* **2016**, *4*, 3487−3493.
(24) Gao, H.; Zhao, L.; Wang, L.; Sun, P.; Lu, H.; Liu, F.; Chuai, X.; Lu, G. Ultrasensitive and Low Detection Limit of Toluene Gas Sensor Based on SnO2-Decorated NiO Nanostructure. *Sens. Actuators, B* **2018**, *255*, 3505−3515.
(25) Zhang, H.-D.; Yan, X.; Zhang, Z.-H.; Yu, G.-F.; Han, W.-P.; Zhang, J.-C.; Long, Y.-Z. Electrospun PEDOT:PSS/PVP Nanofibers for CO Gas Sensing with Quartz Crystal Microbalance Technique. *Int. J. Polym. Sci.* **2016**, *2016*, No. 3021353.
(26) Nalage, S. R.; Mane, A. T.; Pawar, R. C.; Lee, C. S.; Patil, V. B. Polypyrrole−NiO Hybrid Nanocomposite Films: Highly Selective, Sensitive, and Reproducible NO2 Sensors. *Ionics* **2014**, *20*, 1607−1616.
(27) Hwang, S.; Kim, Y. K.; Jeong, S. M.; Choi, C.; Son, K. Y.; Lee, S. Wearable Colorimetric Sensing Fiber Based on Polyacrylonitrile with PdO @ ZnO Hybrids for the Application of Detecting H 2 Leakage. *Text. Res. J.* **2020**, 2198.
(28) Simon, I.; Savitsky, A.; Mülhaupt, R.; Pankov, V.; Janiak, C. Nickel Nanoparticle-Decorated Reduced Graphene Oxide/WO(3) Nanocomposite - a Promising Candidate for Gas Sensing. *Beilstein J. Nanotechnol.* **2021**, *12*, 343−353.
(29) Simon, I.; Haiduk, Y.; Mülhaupt, R.; Pankov, V.; Janiak, C. Selected Gas Response Measurements Using Reduced Graphene Oxide Decorated with Nickel Nanoparticles. *Nano Mater. Sci.* **2021**, *3*, 412−419.
(30) Hapidin, D. A.; Munir, M. M.; Suprijadi; Khairurrijal, K. Development of a New Personal Air Filter Test System Using a Low-Cost Particulate Matter (PM) Sensor. *Aerosol Sci. Technol.* **2020**, *54*, 203−216.
(31) Aria, M. M.; Irajizad, A.; Astaraei, F. R.; Shariatpanahi, S. P.; Sarvari, R. Ethanol Sensing Properties of PVP Electrospun Membranes Studied by Quartz Crystal Microbalance. *Meas. J. Int. Meas. Conf.* **2016**, *78*, 283−288.
(32) Demiroğlu Mustafov, S.; Mohanty, A. K.; Misra, M.; Seydibeyoğlu, M. Ö. Fabrication of Conductive Lignin/PAN Carbon Nanofibers with Enhanced Graphene for the Modified Electrodes. *Carbon N. Y.* **2019**, *147*, 262−275.
(33) Rianjanu, A.; Nugroho, D. B.; Kusumaatmaja, A.; Roto, R.; Triyana, K. A Study of Quartz Crystal Microbalance Modified with Polyvinyl Acetate Nanofiber to Differentiate Short-Chain Alcohol Isomers. *Sens. Bio-Sensing Res.* **2019**, *25*, No. 100294.
(34) Rianjanu, A.; Hasanah, S. A.; Nugroho, D. B.; Kusumaatmaja, A.; Roto, R.; Triyana, K. Polyvinyl Acetate Film-Based Quartz Crystal Microbalance for the Detection of Benzene, Toluene, and Xylene Vapors in Air. *Chemosensors* **2019**, *7*, 20.
(35) Wu, M.; Xie, G.; Zhou, Y.; Tai, H. *A PVP-Based Quartz Crystal Microbalance Sensor for H 2 S Detection*. 2014, *653*, 191−194. doi: DOI: 10.4028/www.scientific.net/AMM.651-653.191.
(36) Priyanto, A.; Hapidin, D. A.; Suciati, T.; Khairurrijal, K. Current Developments on Rotary Forcespun Nanofibers and Prospects for Edible Applications. *Food Eng. Rev.* **2022**, *14*, 435−461.
(37) Rianjanu, A.; Hidayat, S. N.; Julian, T.; Suyono, E. A.; Kusumaatmaja, A.; Triyana, K. Swelling Behavior in Solvent Vapor Sensing Based on Quartz Crystal Microbalance ({QCM}) Coated Polyacrylonitrile ({PAN}) Nanofiber. *IOP Conf. Ser. Mater. Sci. Eng* **2018**, *367*, 12020.
(38) Long, G. L.; Winefordner, J. D. Limit of Detection A Closer Look at the IUPAC Definition. *Anal. Chem.* **1983**, *55*, 712A−724A.
(39) Divya, R.; Manikandan, N.; Vinitha, G. Synthesis and Characterization of Nickel Doped Zinc Selenide Nanospheres for Nonlinear Optical Applications. *J. Alloys Compd.* **2019**, *791*, 601−612.
(40) Dhakate, S. R.; Gupta, A.; Chaudhari, A.; Tawale, J.; Mathur, R. B. Morphology and Thermal Properties of PAN Copolymer Based Electrospun Nanofibers. *Synth. Met.* **2011**, *161*, 411−419.
(41) Liu, Y.; Chae, H. G.; Kumar, S. Gel-Spun Carbon Nanotubes / Polyacrylonitrile Composite Fibers . Part II : Stabilization Reaction Kinetics and Effect of Gas Environment. *Carbon N. Y.* **2011**, *49*, 4477−4486.
(42) Saranya, S.; Dhanapandian, S.; Nagarajan, S.; Suthakaran, S.; Krishnakumar, N. Hydrothermal Synthesis and Characterization of Nanostructured Nickel Diselenide (NiSe2) from the Decomposition of Nickel Acetate Tetrahydrate (Ni(CH3COO)2).4H2O. *Mater. Lett.* **2020**, *277*, No. 128398.
(43) Zhang, C.; Ren, Z.; Yin, Z.; Jiang, L.; Fang, S. Experimental FTIR and Simulation Studies on H-Bonds of Model Polyurethane in Solutions. I: In Dimethylformamide (DMF). *Spectrochim. Acta Part A Mol. Biomol. Spectrosc.* **2011**, *81*, 598−603.
(44) Khalili, R.; Mehdi Sabzehmeidani, M.; Parvinnia, M.; Ghaedi, M. Removal of Hexavalent Chromium Ions and Mixture Dyes by Electrospun PAN/Graphene Oxide Nanofiber Decorated with Bimetallic Nickel-Iron LDH. *Environ. Nanotechnology, Monit. Manag.* **2022**, No. 100750.
(45) Zhao, G.; Li, C.; Wu, X.; Yu, J.; Jiang, X.; Hu, W.; Jiao, F. Reduced Graphene Oxide Modified NiFe-Calcinated Layered Double Hydroxides for Enhanced Photocatalytic Removal of Methylene Blue. *Appl. Surf. Sci.* **2018**, *434*, 251−259.
(46) Mokoena, T. P.; Swart, H. C.; Motaung, D. E. A Review on Recent Progress of P-Type Nickel Oxide Based Gas Sensors: Future Perspectives. *J. Alloys Compd.* **2019**, *805*, 267−294.
(47) Wang, H.; Wang, H.; Ruan, F.; Feng, Q.; Wei, Y.; Fang, J. High-Porosity Carbon Nanofibers Prepared from Polyacrylonitrile Blended with Amylose Starch for Application in Supercapacitors. *Mater. Chem. Phys.* **2023**, *293*, No. 126896.
(48) Hidayat, S. N.; Julian, T.; Rianjanu, A.; Kusumaatmadja, A.; Triyana, K.; Roto Quartz Crystal Microbalance Coated by PAN Nanofibers and PEDOT: PSS for Humidity Sensor. In *2017 International Seminar on Sensors, Instrumentation, Measurement and Metrology (ISSIMM)*; IEEE, 2017, 2017-January, 119−123, DOI: 10.1109/ISSIMM.2017.8124274.
(49) Nugroho, D. B.; Rianjanu, A.; Triyana, K.; Kusumaatmaja, A.; Roto, R. Quartz Crystal Microbalance-Coated Cellulose Acetate Nanofibers Overlaid with Chitosan for Detection of Acetic Anhydride Vapor. *Results Phys.* **2019**, *15*, No. 102680.
(50) Rianjanu, A.; Triyana, K.; Nugroho, D. B.; Kusumaatmaja, A.; Roto, R. Electrospun Polyvinyl Acetate Nanofiber Modified Quartz Crystal Microbalance for Detection of Primary Alcohol Vapor. *Sens. Actuators, A Phys.* **2020**, *301*, No. 111742.
(51) Rianjanu, A.; Roto, R.; Julian, T.; Hidayat, S. N. *Polyacrylonitrile Nanofiber-Based Quartz Crystal*. 2018, 1−11, DOI: 10.3390/s18041150.
(52) Mirzaei, A.; Leonardi, S. G.; Neri, G. Detection of Hazardous Volatile Organic Compounds (VOCs) by Metal Oxide Nanostructures-Based Gas Sensors: A Review. *Ceram. Int.* **2016**, *42*, 15119−15141.
(53) Haghighi, E.; Zeinali, S. Nanoporous MIL-101(Cr) as a Sensing Layer Coated on a Quartz Crystal Microbalance (QCM) Nanosensor to Detect Volatile Organic Compounds (VOCs). *RSC Adv.* **2019**, *9*, 24460−24470.
(54) Triyana, K.; Rianjanu, A.; Nugroho, D. B.; Asari, A. H.; Kusumaatmaja, A.; Roto, R.; Suryana, R.; Wasisto, H. S. A Highly Sensitive Safrole Sensor Based on Polyvinyl Acetate (PVAc) Nanofiber-Coated QCM. *Sci. Rep.* **2019**, *9*, 1−12.
(55) Rong, Q.; Zhang, Y.; Wang, C.; Zhu, Z.; Zhang, J.; Liu, Q. A High Selective Methanol Gas Sensor Based on Molecular Imprinted Ag-LaFeO3 Fibers. *Sci. Rep.* **2017**, *7*, 12110.

https://doi.org/10.1021/acsomega.3c00760
ACS Omega 2023, 8, 13342−13351